Diagn Interv Radiol 2022; DOI: 10.5152/dir.2022.21108

ABDOMINAL IMAGING

REVIEW ARTICLE

Diagnostic value of magnetic resonance imaging features of microvascular invasion in hepatocellular carcinoma: a meta-analysis

Lang Wang
Mimi Jia
Xiaoling Wen
Jiang Shen
Hanfeng Yang

PURPOSE
This systematic review and meta-analysis of conventional enhanced magnetic resonance imaging (MRI) were conducted to evaluate the diagnostic performance of imaging features of microvascular invasion (MVI) prediction in hepatocellular carcinoma (HCC).

METHODS
Relevant studies on diagnosing MVI in HCC by MRI were searched in the MEDLINE, PUBMED, EMBASE, Cochrane library, and Web of Science databases. The pooled mean sensitivity and specificity were calculated using a random effects model. The corresponding positive likelihood ratio (PLR), negative likelihood ratio (NLR), and pooled diagnostic odds ratio (DOR) were calculated. The summary receiver operating characteristic (SROC) curve was used to summarize the overall diagnostic accuracy. Diagnostic performance was evaluated by determining the area under the curve (AUC). Regression analysis by subgroup and sensitivity analysis were used to explore potential sources of heterogeneity.

RESULTS
A total of 19 studies comprising 1920 HCC patients with 2033 tumors were ultimately enrolled. For the signs of the presence of peritumoral enhancement in the arterial phase, peritumoral hypointensity in the hepatobiliary phase, irregular non-smooth margin, and rim-like enhancement in the arterial phase, the pooled sensitivity values, the pooled specificity values, the pooled PLR values, the pooled NLR values, the pooled DOR values, and the values of the AUC of SROC curves were determined.

CONCLUSION
The conventional MRI features for predicting MVI showed poor diagnostic performance in HCC. Only signs of the presence of peritumoral enhancement in the arterial phase showed a moderate diagnostic accuracy.

In hepatocellular carcinoma (HCC), microvascular invasion (MVI), which is considered microscopic evidence of cancer embolism in the portal vein or vascular space lined by endothelial cells, is a prognostic factor for poor overall survival and recurrence after hepatectomy or liver transplantation.[1,2] For patients with HCC who underwent curative surgical resection, detection of MVI plays an important role in clinical decision-making. Subsequent treatment approaches, such as postoperative adjuvant transcatheter arterial chemoembolization, are recently recommended for patients with MVI-positive HCC to prevent recurrence and improve the prognosis.[3,4] Unfortunately, with a high positive incidence rate of up to 57%, MVI can only be confirmed by postoperative pathological examination after extensive resection of the tumor,[5,6] which makes it difficult to predict MVI preoperatively.

As a non-invasive examination, enhanced magnetic resonance imaging (MRI), especially hepatobiliary-specific contrast-enhanced MRI, is currently used for detecting MVI.[7] Incomplete tumor capsules, irregular non-smooth margin, rim-like enhancement on the arterial phase, peritumoral enhancement on the arterial phase, and peritumoral hypointensity on the hepatobiliary phase (HBP) are considered as possible radiographic signs for MVI detection.[8] Rim-like enhancement is defined as the irregular rim-like peripheral hyperintensity

From the Department of Radiology (L.W., X.W., J.S., ✉ sj_scdxhxdsyy@163.com), West China School of Public Health and West China Fourth Hospital, Sichuan University, Chengdu, China; China Outpatient Office (M.J.), West China School of Public Health and West China Fourth Hospital, Sichuan University, Chengdu, China and Department of Radiology (H.Y.), Affiliated Hospital of North Sichuan Medical College, Sichuan, China.

Received 23 December 2020; revision requested 26 January 2021; last revision received 3 May 2021; accepted 17 May 2021.

Publication date: 5 October 2022.

DOI: 10.5152/dir.2022.21108

You may cite this article as: Wang L, Jia M, Wen X, Shen J, Yang H. Diagnostic value of magnetic resonance imaging features of microvascular invasion in hepatocellular carcinoma: A meta-analysis. *Diagn Interv Radiol.* 2022;28(5):428-440.

area of the tumor with hypointensity area in the center of the tumor on the arterial phase enhancement. Peritumoral enhancement is defined as the variable-shaped hyperintensity area outside the tumor in wide contact with the tumor margin on the arterial phase enhancement and iso-intensity area on the delayed phase. Peritumoral hypointensity is defined as a flame-like or "V-shaped" hypointense area outside the tumor margin on the HBP. Irregular non-smooth margin is defined as an indistinct or irregular tumor margin with a budding portion.[9] However, the diagnostic performance, with respect to the accuracy, is still controversial. The systematic evaluation of the image prediction of MVI in HCC has been reported in recent studies[10-13] with variable pooled results of diagnostic values. There were obvious methodological differences such as different examination types [computed tomography (CT), ultrasound, MRI, or positron emission tomography/CT (PET/CT)] and confused methodology (conventional MRI or using radiomics) among these studies. In addition, the radiographic signs selection in the MRI subgroup was different, so it is uncertain for comparing the diagnostic performance of the specific image signs on MRI. Therefore, we conducted a systematic review and meta-analysis of conventional enhanced MRI to evaluate the diagnostic performance of imaging features for MVI prediction in HCC.

Methods

Search strategy

This study was conducted based on the Preferred Reporting Items for Systematic Reviews and Meta-Analyses–Diagnostic Test Accuracy Statement.[14] Relevant studies on the diagnosis of MVI in HCC by MRI were searched in the MEDLINE, PUBMED, EMBASE, Cochrane Library, and Web of Science databases through December 12, 2020. The search terms were as follows: [(microvascular invasion) OR (microvessel invasion) OR (MVI)] AND [(magnetic resonance imaging) OR (MR imaging) OR (MRI)] combined with terms of [(hepatocellular) OR (HCC)]. The references to the searched literature were also screened to identify the relevant studies. In addition, manual identification was performed to expand the search of the literature. There was no limitation of language and design in the analysis. For this meta-analysis, all the data were based on published articles, so neither ethical approval nor informed consent was required. Two reviewers independently performed the literature search and selection. When there was any disagreement, they were required to discuss it with a third reviewer and then reach a consensus.

Eligibility criteria

Studies were included when they met the following inclusion criteria: (1) evaluated MVI in HCC using MRI and found features, such as rim-like enhancement on the arterial phase, peritumoral enhancement on the arterial phase, peritumoral hypointensity on the HBP, or irregular non-smooth margin; (2) patients underwent MRI before hepatectomy or liver transplantation; (3) confirmed HCC and MVI in HCC patient by pathologic diagnosis after surgery; (4) data can be extracted from a 2 × 2 table. Studies were excluded if they met the following exclusion criteria: (1) HCC patients underwent radiofrequency

Main points

- We summarized four of the most common magnetic resonance imaging (MRI) signs for microvascular invasion (MVI) in hepatocellular carcinoma (HCC).
- A systematic evaluation of the diagnostic performance was performed to predict MVI in HCC using conventional enhanced MRI (non-functional or radiomics) of each sign.
- The diagnostic performance of conventional enhanced MRI was not good, and all the signs showed low-moderate diagnostic accuracy.

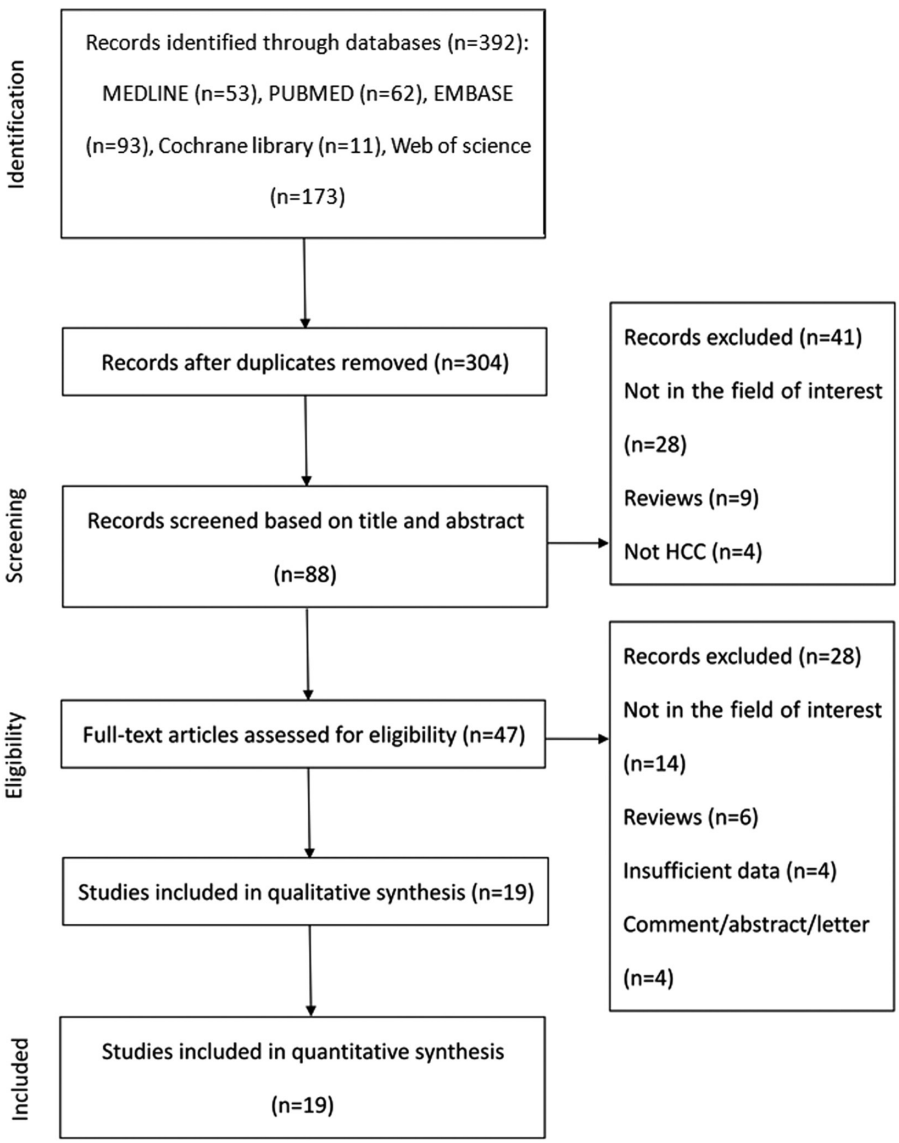

Figure 1. Flow diagram of studies selection.

ablation, transarterial chemoembolization, chemotherapy, or other systematic therapy before surgery; (2) HCC patients underwent MVI evaluation using a radiomics model or functional MRI without imaging features; (3) meeting papers, case reports, reviews, comments, or reference abstracts; (4) insufficient data or unavailability of full-text.

Data extraction and quality assessment

The following items were extracted: (1) study characteristics including authors, publication year, mean age, number of patients, number of tumors, tumor size, interval between MRI examination and pathological diagnosis, scanning mode (using hepatobiliary MRI or not), and magnetic field intensity (1.5 T and/or 3.0 T);

Table 1. Study characteristics and diagnostic data of MRI finding

Study	Year	Size <5 cm only	Interval	Scanning mode*	Magnetic field intensity	Patients (tumors)	Age	MRI finding	TP	FP	FN	TN
Wang X[16]	2020	Yes	≤1 month	Yes	3.0T	61 (61)	56.0	Peritumor hypointensity	14	40	5	2
Zhang L[17]	2020	No	≤1 month	Yes	1.5T	164 (164)	55.9	Peritumoral enhancement	14	5	47	98
								Peritumor hypointensity	31	92	30	11
								Irregular non-smooth margin	41	45	20	58
								Rim-like enhancement	38	39	23	64
Zhang T[18]	2020	No	≤1 month	No	3.0T	128 (136)	52.7	Peritumoral enhancement	14	4	47	71
								Irregular non-smooth margin	38	28	23	47
Lee S[19]	2020	No	>1 month	Yes	1.5T + 3.0T	122 (122)	54.0	Peritumor hypointensity	16	5	5	96
Lu XY[20]	2020	No	≤1 month	Yes	3.0T	102 (102)	57.5	Peritumor hypointensity	20	6	11	65
Chou YC[21]	2019	No	≤1 month	Yes	1.5T	114 (114)	59.1	Peritumor hypointensity	23	57	16	18
								Irregular non-smooth margin	12	18	27	57
								Rim-like enhancement	14	13	25	62
Rhee H[22]	2019	No	>1 month	No	1.5T + 3.0T	84 (84)	55.0	Rim-like enhancement	24	18	9	33
Ahn SJ[23]	2018	No	≤1 month	Yes	1.5T + 3.0T	179 (179)	56.7	Peritumoral enhancement	31	33	37	78
								Peritumor hypointensity	33	26	35	85
								Irregular non-smooth margin	46	46	22	65
Huang M[24]	2018	No	≤1 month	Yes	3.0T	60 (66)	52.2	Peritumoral enhancement	11	10	6	39
								Peritumor hypointensity	5	14	12	35
								Irregular non-smooth margin	17	38	0	11
Kim AY[25]	2018	No	>1 month	Yes	3.0T	100 (100)	52.5	Peritumoral enhancement	8	2	47	43
								Peritumor hypointensity	13	1	42	44
								Irregular non-smooth margin	42	17	13	28
Lee S[26]	2017	Yes	≤1 month	Yes	3.0T	197 (197)	54.9	Peritumoral enhancement	34	16	29	118
								Peritumor hypointensity	43	123	20	11
								Irregular non-smooth margin	44	44	19	92
								Rim-like enhancement	18	13	45	121
Zhou XM[27]	2017	No	≤1 month	No	3.0T	107 (107)	56.5	Peritumoral enhancement	9	14	25	59
								Irregular non-smooth margin	27	36	4	34
Yoneda N[28]	2017	No	>1 month	Yes	1.5T + 3.0T	68 (77)	65.2	Peritumor hypointensity	20	7	23	27
Xu P[29]	2014	Yes	≤1 month	No	1.5T	92 (109)	53.2	Peritumoral enhancement	10	10	29	60
Ahn SY[30]	2014	No	≤1 month	Yes	1.5T + 3.0T	51 (78)	51.9	Peritumoral enhancement	6	4	12	56
								Peritumor hypointensity	2	2	16	58
								Irregular non-smooth margin	11	20	7	40
Kim KA[31]	2012	No	≤1 month	Yes	3.0T	104 (104)	55.0	Peritumor hypointensity	37	41	23	3
Chandarana H[32]	2011	No	>1 month	No	1.5T + 3.0T	60 (102)	57.9	Irregular non-smooth margin	41	42	12	7
Ariizumi S[33]	2011	Yes	≤1 month	Yes	1.5T	61 (61)	67.0	Irregular non-smooth margin	10	14	1	36
Kim H[34]	2009	No	≤1 month	Yes	1.5T	66 (70)	55.1	Peritumoral enhancement	28	14	7	21
								Irregular non-smooth margin	19	8	16	27

*Scanning mode: hepatobiliary MRI or not.
MRI, magnetic resonance imaging; TP, true positive; FP, false positive; FN, false negative; TN, true negative.

(2) data of true positives (TP), false positives (FP), false negatives (FN), and true negatives (TN) for rim-like enhancement, peritumoral enhancement, peritumoral hypointensity, or irregular non-smooth margin. In addition, the quality of eligible studies was assessed using the Quality Assessment of Diagnostic Accuracy Studies-2 (QUADAS-2) tool. The data extraction and quality assessment were independently performed by 2 reviewers. When there was any disagreement, they were required to discuss it with a third reviewer and then reach a consensus.

Statistical analysis

The pooled results of the sensitivity, specificity, and corresponding 95% CI were calculated by a random effects model. The positive likelihood ratio (PLR), negative likelihood ratio (NLR), and pooled diagnostic odds ratio (DOR) were also calculated. The summary receiver operating characteristic (SROC) curve was used to summarize the overall diagnostic accuracy. Diagnostic performance was evaluated by determining the area under the curve (AUC). An AUC of more than 0.9 was considered to be of high diagnostic accuracy.[15] The heterogeneity was assessed by the I^2 statistic test, and an I^2 value higher than 0.5 was considered to indicate significant study heterogeneity. A *P*-value of less than .05 indicated statistical significance. The threshold effect was detected using Spearman correlation between the sensitivity and FP rate. Regression analysis by subgroup and sensitivity analysis were used to find potential sources of heterogeneity. The parameters of subgroup patients included: tumor size (the size of all tumors was less than 5 cm only or not), mean interval between MRI examination and pathological diagnosis (≤1 month vs. >1 month), magnetic field intensity (unitary field of 1.5T or 3.0T vs. both fields of 1.5T and 3.0T), and using hepatobiliary-specific contrast agent or not. The graphical sensitivity analysis consisted of the following 4 parts: (a) quantile plot of goodness-of-fit; (b) quantile plot of bivariate normality; (c) spike plot of influence analysis using Cook's distance; and (d) scatter plot for outlier detection. The publication bias was evaluated by Deeks' funnel plot. The Stata software version 13.0 (StataCorp) and Meta-Disc software version 1.4 (Clinical Biostatistics Unit, Ramon y Cajal Hospital) were used for statistical analysis (Meta-Disc was used for evaluating the threshold effect only).

Results

According to the used strategies, a total of 392 studies were identified. After removing the duplicated records, we excluded the studies by title and abstract screening. Then, full text assessment of the remaining articles was performed. A flow diagram of the whole process is shown in Figure 1. Ultimately, 19 studies,[16-34] comprising 1920 HCC patients with 2033 tumors, were included in the analysis.

Study characteristics and diagnostic data are summarized in Table 1. Eighteen studies[16-19,21-34] were in English and 1 was in Chinese.[20] Fourteen of the included studies[16,17,19-21,23-26,28,30,31,33,34] used hepatobiliary MRI, and 6 used both 1.5T and 3.0T for magnetic resonance scanning.[19,22,23,28,30,32] Four studies[16,26,29,33] only included tumors with size below 5 cm. A total of 10 studies[17,18,23-27,29,30,34] reported the MRI finding of peritumoral enhancement on the arterial phase, 12[16,17,19-21,23-26,28,30,31] reported peritumoral hypointensity on the HBP, another 12[17,18,21,23-27,30,32-34] reported irregular non-smooth margin, and 4[17,21,22,26] reported rim-like enhancement on the arterial phase. The results of the quality assessment using the QUADAS-2 tool are shown in Figure 2 and revealed that the quality of the included studies was moderate.

For the signs of the presence of peritumoral enhancement in the arterial phase, the pooled sensitivity was 0.37 (95% CI: 0.25-0.51) with an I^2 value of 87.06% (95% CI: 80.30%-93.82%). The pooled specificity was 0.87 (95% CI: 0.79-0.92) with an I^2 value of 85.35% (95% CI: 77.42%-93.27%) (Figure 3a). The pooled PLR was 2.86 (95% CI: 2.03-4.04) with an I^2 value of 23.93% (95% CI: 23.93%-87.07%). The pooled NLR was 0.72 (95% CI: 0.61-0.85) with an I^2 value of 70.40% (95% CI: 51.19%-89.62%). The pooled DOR was 3.95 (95% CI: 2.58-6.05) with an I^2 value of 98.73% (95% CI: 98.41%-99.06%). The AUC was 0.72 (95% CI: 0.68-0.76) (Figure 3b). A significant threshold effect was found with Spearman correlation coefficients of 0.839 ($P = .002$).

For the sign of the presence of peritumoral hypointensity on HBP, the pooled sensitivity was 0.51 (95% CI: 0.40-0.62) with an I^2 value of 82.88% (95% CI: 74.12%-91.65%). The pooled specificity was 0.60 (95% CI: 0.26-0.86) with an I^2 value of 97.90% (95% CI: 97.33%-98.48%) (Figure 4a). The pooled

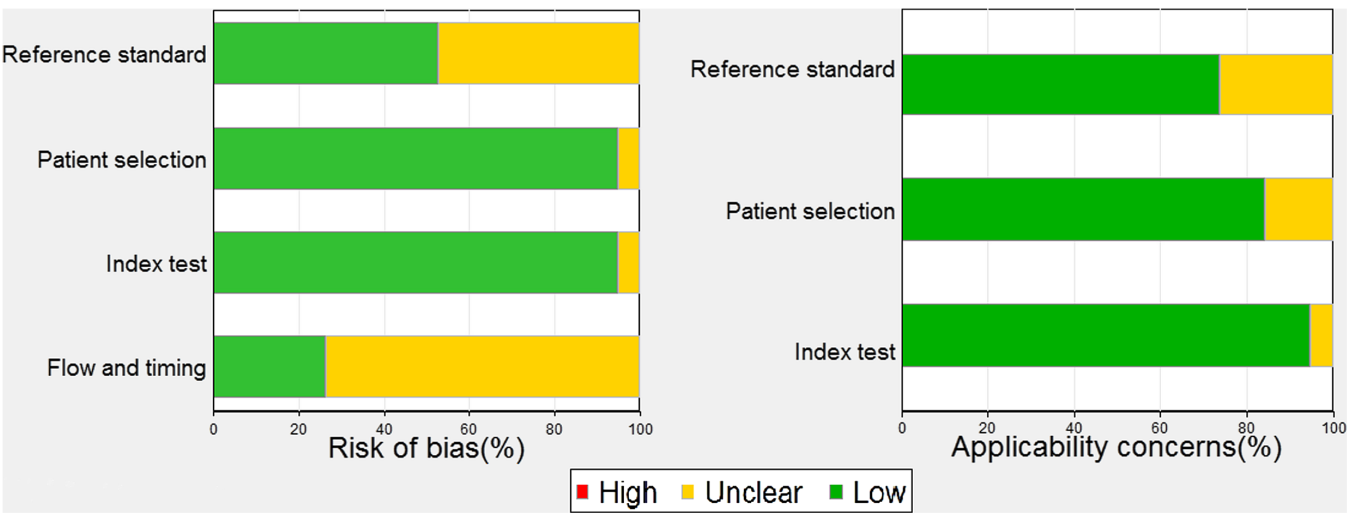

Figure 2. The summarized results for quality assessment of enrolled studies according to QUADAS-2 tools. QUADAS-2, Quality Assessment of Diagnostic Accuracy Studies-2.

PLR was 1.27 (95% CI: 0.60-2.70) with an I^2 value of 92.37% (95% CI: 92.37%-96.49%). The pooled NLR was 0.82 (95% CI: 0.51-1.32) with an I^2 value of 89.57% (95% CI: 84.92%-94.22%). The pooled DOR was 1.56 (95% CI: 0.46-5.31) with an I^2 value of 100.00% (95% CI: 100%-100%). The AUC was 0.53 (95% CI: 0.49-0.58) (Figure 4b). The threshold effect was not determined ($P = .106$).

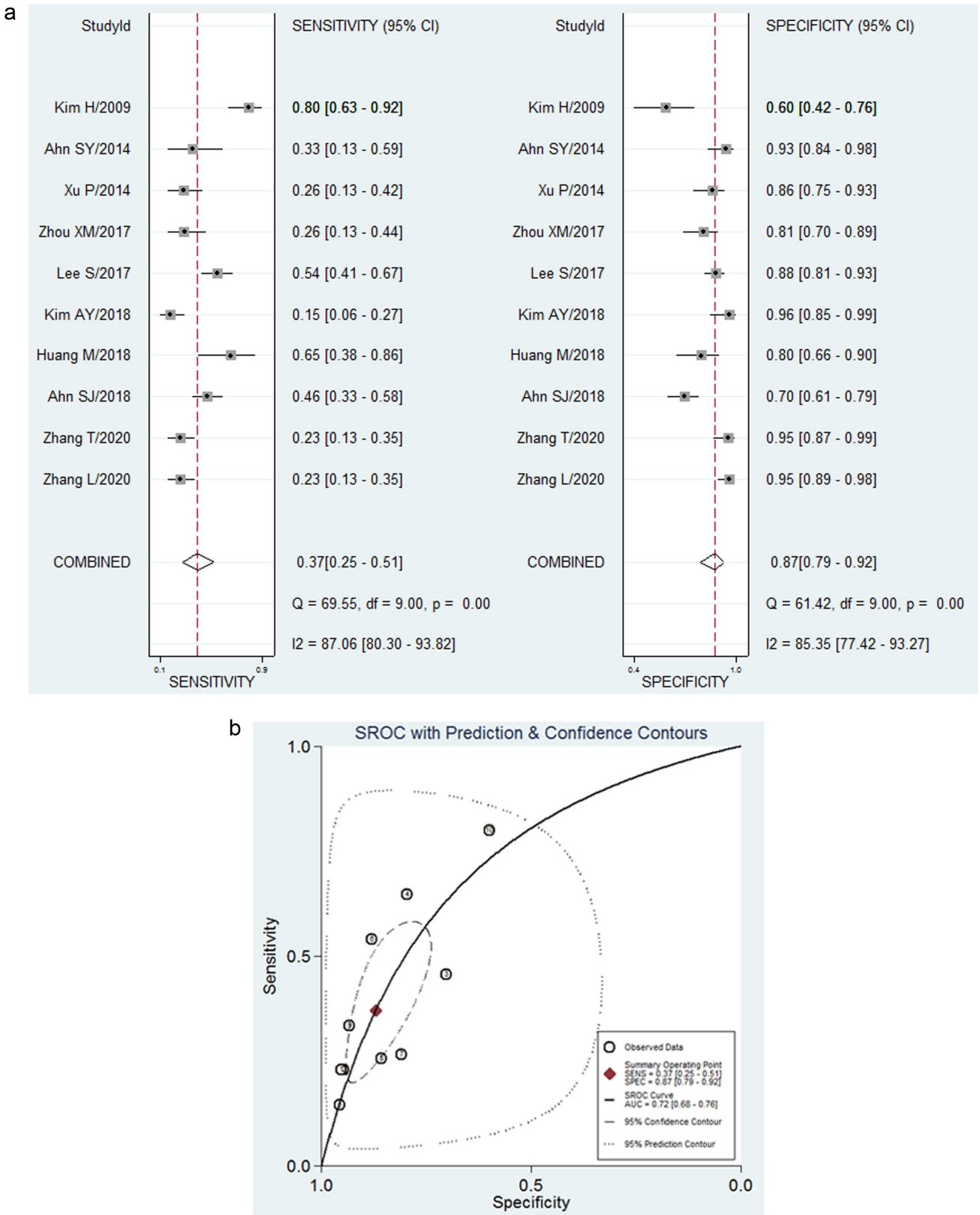

Figure 3. Diagnostic performance of peritumoral enhancement on arterial phase for MVI prediction in HCC. **(a)** The coupled forest plots; **(b)** The SROCs. MVI, microvascular invasion; HCC, hepatocellular carcinoma; SROC, summary receiver operating characteristic.

For the sign of the presence of irregular non-smooth margin, the pooled sensitivity was 0.71 (95% CI: 0.60-0.79) with an I^2 value of 77.70% (95% CI: 65.44%-89.96%). The pooled specificity was 0.57 (95% CI: 0.46-0.68) with an I^2 value of 88.29% (95% CI: 82.89-93.68%) (Figure 5a). The pooled PLR was 1.65 (95% CI: 1.35 - 2.02) with an I^2 value of 73.38% (95% CI: 73.38-91.50%).

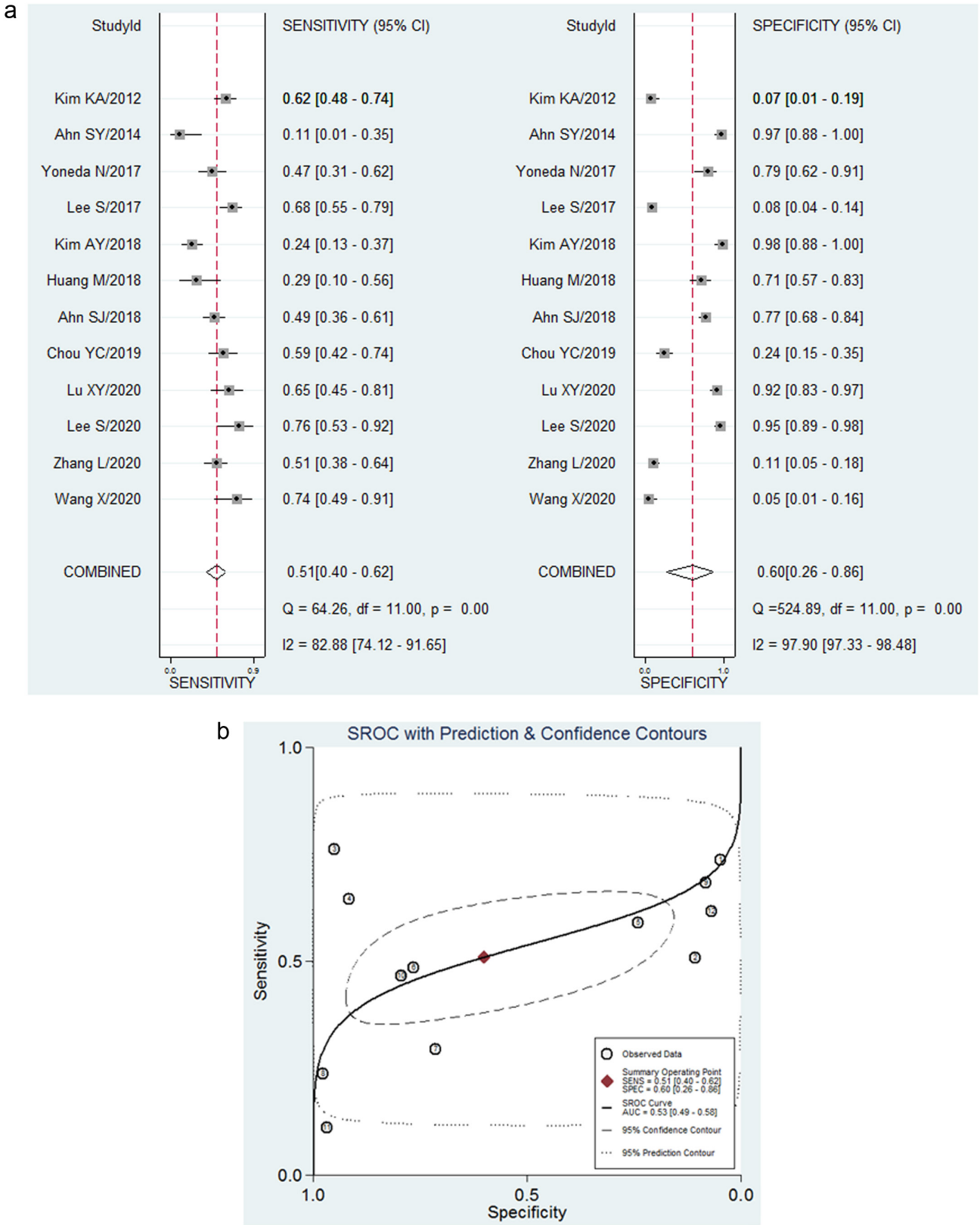

Figure 4. Diagnostic performance of peritumoral hypointensity on HBP for MVI prediction in HCC. **(a)** The coupled forest plots; **(b)** The SROCs. HBP, hepatobiliary phase.

The pooled NLR was 0.51 (95% CI: 0.40-0.66) with an I^2 value of 65.71% (95% CI: 44.72%-86.70%). The pooled DOR was 3.21 (95% CI: 2.18-4.71) with an I^2 value of 99.95% (95% CI: 99.95- 99.96%). The AUC was 0.69 (95% CI: 0.65-0.73) (Figure 5b). A significant threshold effect was found with Spearman correlation coefficients of 0.601 ($P = .039$).

For the sign of the presence of rim-like enhancement in the arterial phase, the pooled sensitivity was 0.49 (95% CI: 0.31-0.67) with an I^2 value of 87.95% (95%

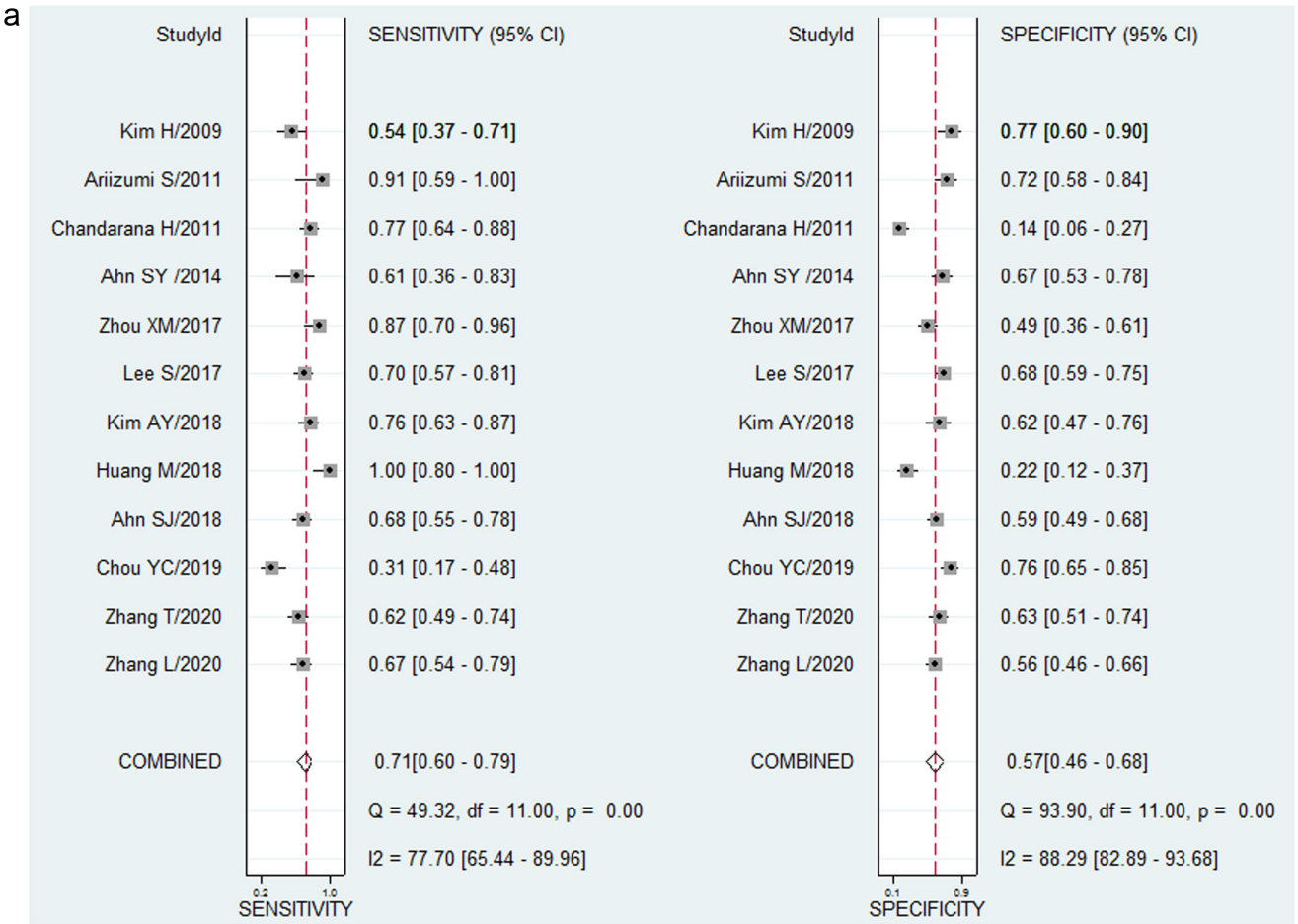

Figure 5. Diagnostic performance of irregular non-smooth margin for MVI prediction in HCC. **(a)** The coupled forest plots; **(b)** The SROC.

CI: 77.58%-98.32%). The pooled specificity was 0.77 (95% CI: 0.62-0.88) with an I^2 value of 90.65% (95% CI: 83.12%-98.17%) (Figure 6a). The pooled PLR was 2.14 (95% CI: 1.57-2.92) with an I^2 value of 0.00% (95% CI: 0.00%-100%). The pooled NLR was 0.66 (95% CI: 0.52-0.84) with an I^2 value of 59.62% (95% CI: 15.27%-100%). The pooled DOR was 3.25 (95% CI: 2.19-4.82) with an I^2 value of 49.02% (95% CI: 0%-100%). The AUC was 0.69 (95% CI: 0.65-0.73) (Figure 6b). The threshold effect was not determined ($P = .200$).

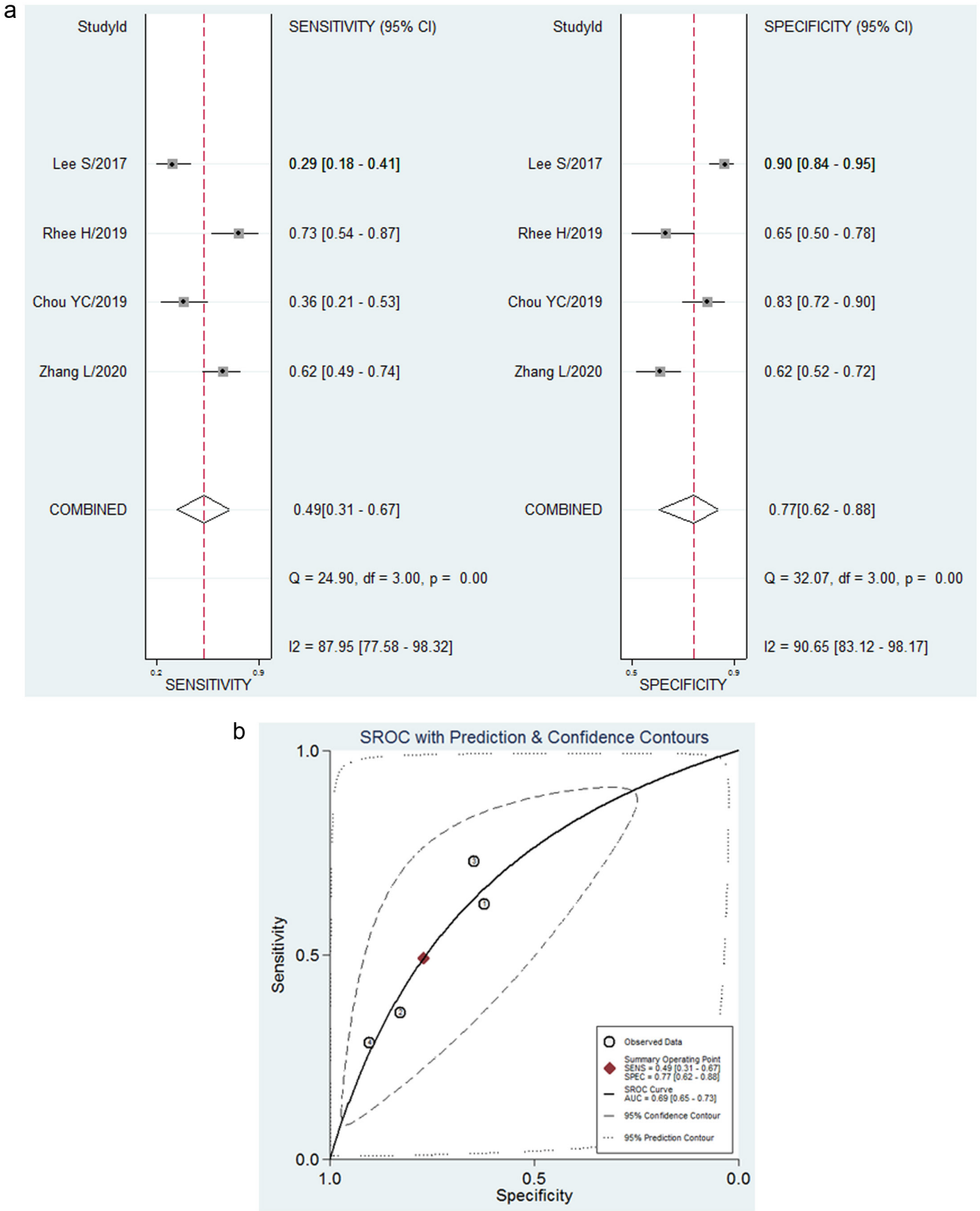

Figure 6. Diagnostic performance of rim-like enhancement on the arterial phase for MVI prediction in HCC. **(a)** The coupled forest plots; **(b)** the SROCs.

Significant study heterogeneity was found for each sign predicting the presence of MVI by MRI. Thus, we performed meta-regression and subgroup analysis for peritumoral enhancement, peritumoral hypointensity, and irregular non-smooth margin (Table 2). The potential source of heterogeneity for peritumoral hypointensity was detected by the non-threshold effect. The subgroup of larger tumors (size >5 cm) showed a higher pooled specificity of 0.74 (95% CI: 0.49-0.98, $P < .01$). The subgroup of longer interval (>1 month) showed a higher pooled specificity of 0.95 (95% CI: 0.83-1.00, $P = .02$). The non-unitary field group showed a higher pooled specificity of 0.91 (95% CI: 0.74-1.00). The diagnostic values in the signs of peritumoral enhancement and irregular non-smooth margin were not changed in the use of a hepatobiliary-specific contrast agent ($P > .05$).

Since only 4 studies included rim-like enhancement, meta-regression analysis was not performed for rim-like enhancement. Accordingly, we performed a sensitivity analysis for this feature to investigate the source of heterogeneity. As for the potential heterogeneity of peritumoral enhancement and irregular non-smooth margin by threshold effect, further sensitivity analysis was also conducted (Figure 7). Each of the included studies showed little impact on the pooled outcomes according to the quantile plot for goodness-of-fit and chi-square plot for bivariate normality. For the peritumoral enhancement and irregular non-smooth margin, the influence analysis and outlier detection showed that few studies affect the effect model, which might be the potential heterogeneity. Additionally, there was no significant impact on the pooled estimates when they were removed. Thus, we concluded that this effect model is stable. For rim-like enhancement, we found no outlier studies by influence analysis and outlier detection. Thus, we concluded that the source of heterogeneity for this feature was unclear, indicating that the pooled results must be viewed with caution.

No significant publication bias was detected by Deek's funnel plot (Figure 8). The number of included studies was small in the MRI finding of rim-like enhancement; thus, we did not assess the publication bias for this feature.

Table 2. The results of meta-regression analysis and subgroup analysis

Parameter	Category	Study number	Sensitivity (95% CI)	Specificity (95% CI)
Peritumoral enhancement				
Size <5 cm only	Yes	2	0.40 (0.11-0.70)	0.88 (0.75-1.00)
	No	8	0.36 (0.21-0.51)	0.87 (0.79-0.94)
Interval ≤1 month	Yes	9	0.40 (0.28-0.53)	0.86 (0.79-0.92)
	No	1	0.14 (−0.05 to 0.34)	0.96 (0.88-1.00)
Unitary field	Yes	8	0.37 (0.22-0.52)	0.88 (0.81-0.94)
	No	2	0.36 (0.06-0.66)	0.83 (0.66-1.00)
Hepatobiliary- specific contrast	Yes	7	0.43 (0.28-0.58)	0.87 (0.79-0.95)
	No	3	0.25 (0.07-0.43)	0.88 (0.77-0.99)
Peritumor hypointensity				
Size <5 cm only	Yes	2	0.71 (0.51-0.91)	0.06 (-0.10-0.21)*
	No	10	0.47 (0.37-0.57)	0.74 (0.49-0.98)*
Interval ≤1 month	Yes	9	0.52 (0.39-0.65)	0.40 (0.07-0.73)*
	No	3	0.46 (0.23-0.68)	0.95 (0.83-1.00)*
Unitary field	Yes	8	0.54 (0.41-0.67)	0.36 (0.03-0.69)*
	No	4	0.45 (0.26-0.63)	0.91 (0.74-1.00)*
Irregular non-smooth margin				
Size <5 cm only	Yes	2	0.75 (0.53-0.91)	0.69 (0.46-0.92)
	No	10	0.70 (0.59-0.80)	0.55 (0.43-0.66)
Interval ≤1 month	Yes	10	0.69 (0.58-0.81)	0.61 (0.50-0.72)
	No	2	0.78 (0.58-0.97)	0.36 (0.12-0.60)
Unitary field	Yes	9	0.71 (0.59-0.83)	0.61 (0.49-0.73)
	No	3	0.69 (0.49-0.90)	0.46 (0.24-0.69)
Hepatobiliary- specific contrast	Yes	9	0.69 (0.57-0.81)	0.62 (0.51-0.74)
	No	3	0.76 (0.59-0.92)	0.42 (0.21-0.62)

*P-value < .05.

Discussion

We performed a systematic evaluation of the diagnostic accuracy of four specific MRI signs for the presence of features, which are widely used for the prediction of MVI in HCC with discrepancy. According to the results of our analyses, the diagnostic performance of MRI features, including peritumoral enhancement, peritumoral hypointensity, irregular non-smooth margin and rim-like enhancement, was not satisfactory. In fact, only the sign for peritumoral enhancement on the arterial phase had a moderate diagnostic accuracy for MVI in HCC with an AUC of 0.72, which was consistent with studies by Hu et al.[11] This sign was observed when the hemodynamic abnormality caused by MVI involved the hepatic tissue around the tumor, which led to a decrease of the portal blood supply and an increase of the hepatic arterial blood supply in the arterial phase.[35,36] The peritumoral hypointensity on the HBP had the worst diagnostic performance in this study. The subgroup analysis revealed that a tumor size larger than 5 cm was an indicator of the higher specificity of this sign to predict the MVI in HCC. Tumor size was an important predictive factor of MVI,[13] indicating that it affected the diagnostic accuracy to a certain extent. The mechanisms of sign formation were as follows: (1) the uptake of the extracellular contrast agent by peritumoral hepatocyte was decreased due to the hepatic cell injury; and (2) the contrast agent perfusion detected was associated with cancer embolism of the portal vein.[37,38] This sign was considered a moderate predictive factor for MVI in a previous systematic review[11] with a DOR of 10.62. However, the size was small, and the pooled analysis was not statistically significant. Thus, we should be cautious to explain their results. The irregular non-smooth margin, which indicated infiltrative growth and protruded into the peritumoral hepatic tissue, exhibited equivalent great diagnostic power as in previous studies.[10,39]

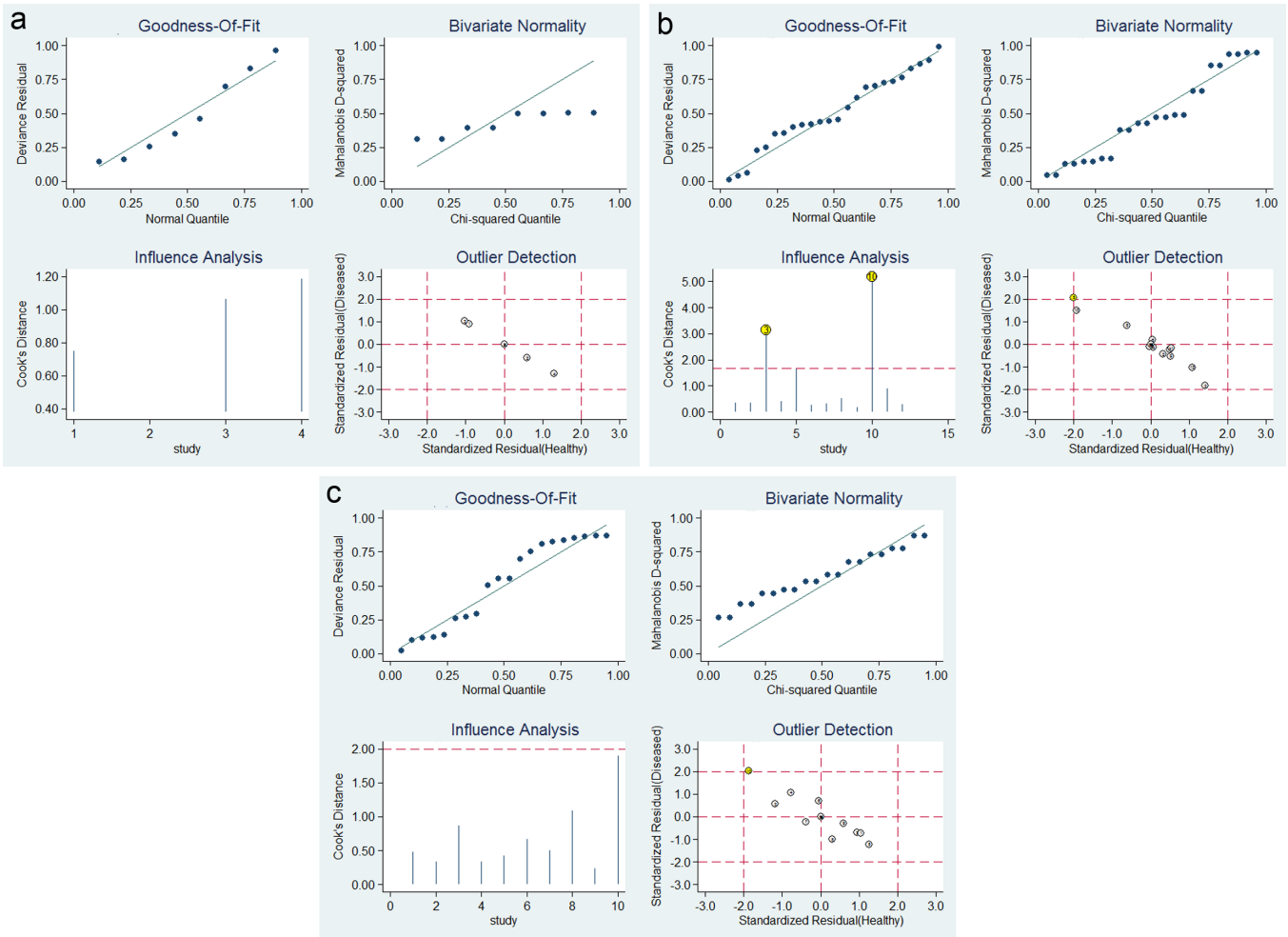

Figure 7. The graphical sensitivity analysis. **(a)** Rim-like enhancement on arterial phase; **(b)** irregular non-smooth margin; **(c)** peritumoral enhancement on arterial phase.

Our pooled results showed similar sensitivity and a lower specificity than the results reported by Hu et al.[10] We assumed that differences in imaging methods and the number of studies led to this divergence. Rim-like enhancement (especially irregular pattern) on the arterial phase is considered a rare sign of HCC with poorer differentiation and more aggressive growth.[22] Only a few of the included studies focused on this sign, and no previous systematic review has evaluated its diagnostic power. However, according to our pooled results, this sign had a poor diagnostic accuracy for predicting MVI.

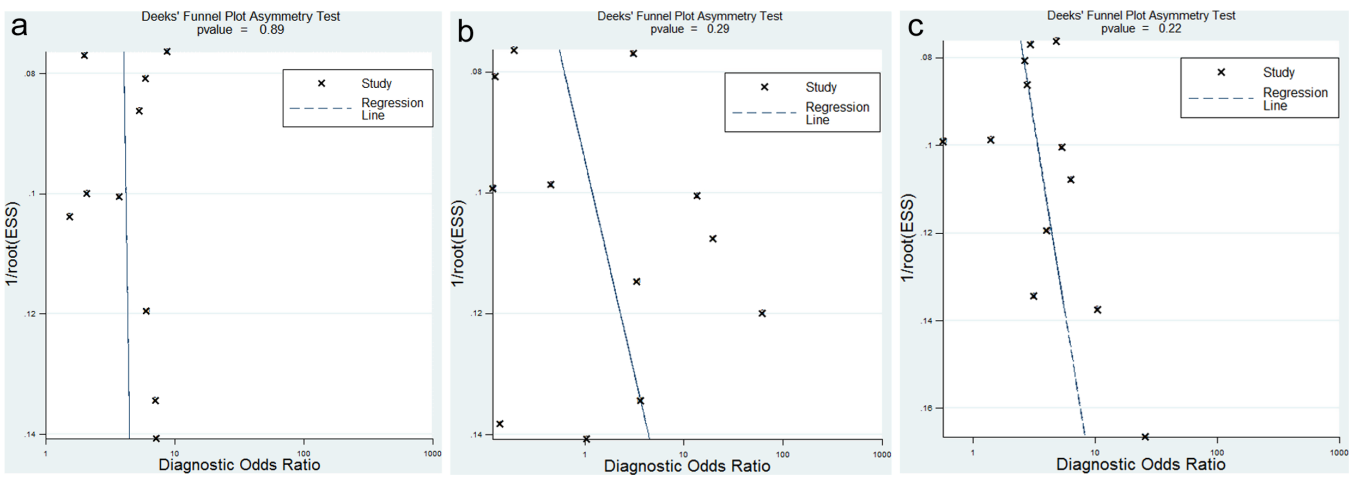

Figure 8. The evaluation of publication bias using Deek's funnel plots. **(a)** Peritumoral enhancement on arterial phase; **(b)** peritumoral hypointensity on HBP; **(c)** irregular non-smooth margin.

Compared to the four signs in our study, other MRI signs that appeared in HCC, such as the mosaic sign, absence of fat in mass, and radiological tumor capsule in Liver Imaging Reporting and Data System (LI-RADS), also showed controversial diagnostic power and independent prediction of recurrence in the high-risk patients with LI-RADS 5 HCC.[13,40,41] A diagnostic meta-analysis[13] for the signs of incomplete radiological tumor capsule and absent radiological tumor capsule showed pooled DORs of 1.85 and 0.90, respectively, for predicting MVI in HCC. In their MRI subgroup, the diagnostic accuracy was not significantly improved compared with the pooled results of the CT group. Based on their results, these two signs had a worse diagnostic performance than the rim-like enhancement, peritumoral enhancement, peritumoral hypointensity, and irregular non-smooth margin. As for the sign of absence of fat in mass, a systematic review[42] indicated that the presence of fat in mass was associated with a negative MVI in HCC. However, the sensitivity, specificity, and DOR results were not calculated, so the diagnostic power was unclear. For signs of peritumoral enhancement and irregular non-smooth margin, the diagnostic performance was not significantly increased with the use of a hepatobiliary-specific contrast agent. This was because, we concluded, those two image signs were not assessed on the HBP. The arterial phase and early portal venous phase enhancement curves for both tumor and liver were similar after the injection of different types of contrast agent.[37] Moreover, the diagnostic performance of rim-like enhancement influenced by the chosen contrast material was not evaluated in our study, because regression analysis by the subgroup was not applicable for this part.

It seemed like the image signs in conventional enhanced MRI did not have a good diagnostic performance. In recent years, the studies using radiomics tools to predict MVI on the image have been reported with various models and different diagnostic accuracy.[43-45] A systematic review[12] revealed a pooled sensitivity of 0.78 and a pooled specificity of 0.78, which indicated a good diagnostic performance using radiomics tools. Another promising method for predicting MVI on images was functional MRI, including diffusion weight image, intravoxel incoherent motion, and T1 mapping.[46-48] Huang et al.[12] found a moderate-good diagnostic accuracy of functional MRI for predicting MVI in HCC. However, they did not distinguish the image modalities (PET/CT was included in their study). Thus, further systematic evaluation of functional MRI of HCC is necessary to determine its diagnostic power for detecting MVI. Other conventional imaging modalities, such as multi-detector CT (MDCT) or ultrasound, were also used for MVI prediction in HCC. In a previous study,[10] MDCT showed an even higher sensitivity in the sign of non-smooth margin than that of MRI. Although MDCT can generally evaluate the radiographic signs of HCC with a shorter scanning time, MRI showed a higher resolution, and hepatobiliary-specif ic contrast enhancement increased the positive finding for small tumors. Contrast-enhanced ultrasound (CEUS) was recently used for MVI evaluation in HCC.[49] The washout sign on CEUS was proved to be correlated with MVI. However, a diagnostic test was not performed. Because the ultrasound exploration was operator-dependent and could be affected by the tumor location in the liver, we believed that preoperative MVI prediction using CEUS needed to be viewed with caution in HCC.

Our study had a number of limitations. First, there was notable heterogeneity in some parts, whether caused by the threshold effect or the non-threshold effect. However, a further sensitivity analysis was performed to demonstrate the stability of the effect models. Some of the included studies had inadequate clinical characteristics; thus, we were unable to perform a more detailed subgroup analysis and meta-regression. Second, most of the included studies did not evaluate the reliability, so the potential influence of diagnostic power caused by inter-observer disagreement was unclear. Finally, we only performed a systematic evaluation for each of the 4 MRI signs to determine which one had the best diagnostic accuracy. More attention needs to be paid to studies on the combination of different MRI signs to predict the presence of MVI in HCC patients.

In conclusion, the MRI signs of features, such as irregular non-smooth margin, rim-like enhancement, peritumoral enhancement, and peritumoral hypointensity on the HBP, had unsatisfactory diagnostic performances in the prediction of MVI in HCC. Only the sign of peritumoral enhancement on the arterial phase had a moderate diagnostic accuracy for MVI prediction, while the sign of peritumoral hypointensity on the HBP had the worst diagnostic performance in this study. Considering the importance of MVI prediction in HCC, improvement of the diagnostic accuracy using MRI signs can be a potential aspect for future research.

Acknowledgments

The authors would like to thank Dr. Yofre C. and Dr. Jason Qee for the language editing.

Conflict of interest disclosure

The authors declared no conflicts of interest.

References

1. Du M, Chen L, Zhao J, et al. Microvascular invasion (MVI) is a poorer prognostic predictor for small hepatocellular carcinoma. *BMC Cancer*. 2014;14:38. [CrossRef]
2. Zhang XP, Wang K, Wei XB, et al. An Eastern Hepatobiliary Surgery Hospital microvascular invasion scoring system in predicting prognosis of patients with hepatocellular carcinoma and microvascular invasion After R0 liver resection: a large-scale, multicenter study. *Oncologist*. 2019;24(12):e1476-e1488. [CrossRef]
3. Wang H, Du PC, Wu MC, Cong WM. Postoperative adjuvant transarterial chemoembolization for multinodular hepatocellular carcinoma within the Barcelona Clinic Liver Cancer early stage and microvascular invasion. *Hepatobiliary Surg Nutr*. 2018;7(6):418-428. [CrossRef]
4. Sun JJ, Wang K, Zhang CZ, et al. Postoperative Adjuvant Transcatheter Arterial Chemoembolization After R0 Hepatectomy Improves Outcomes of Patients Who have Hepatocellular Carcinoma with Microvascular Invasion. *Ann Surg Oncol*. 2016;23(4):1344-1351. [CrossRef]
5. Rodríguez-Perálvarez M, Luong TV, Andreana L, Meyer T, Dhillon AP, Burroughs AK. A systematic review of microvascular invasion in hepatocellular carcinoma: diagnostic and prognostic variability. *Ann Surg Oncol*. 2013;20(1):325-339. [CrossRef]
6. Chen J, Zhou J, Kuang S, et al. Liver imaging reporting and data system Category 5: MRI predictors of microvascular invasion and recurrence After hepatectomy for hepatocellular carcinoma. *AJR Am J Roentgenol*. 2019;213(4):821-830. [CrossRef]
7. Joo I, Kim SY, Kang TW, et al. Radiologic-path ologic correlation of hepatobiliary phase hypointense nodules without arterial phase hyperenhancement at gadoxetic acid-enhanced MRI: A multicenter study. *Radiology*. 2020;296(2):335-345. [CrossRef]
8. Wei H, Jiang H, Liu X, et al. Can LI-RADS imaging features at gadoxetic acid-enhanced MRI predict aggressive features on pathology of single hepatocellular carcinoma? *Eur J Radiol*. 2020;132:109312. [CrossRef]
9. Min JH, Lee MW, Park HS, et al. Interobserver variability and diagnostic performance of gadoxetic acid–enhanced MRI for predicting microvascular invasion in hepatocellular carcinoma. *Radiology*. 2020;297(3):573-581. [CrossRef]

10. Hu H, Zheng Q, Huang Y, et al. A non-smooth tumor margin on preoperative imaging assesses microvascular invasion of hepatocellular carcinoma: a systematic review and meta-analysis [sci rep]. *Sci Rep*. 2017;7(1):15375. [CrossRef]
11. Hu HT, Shen SL, Wang Z, et al. Peritumoral tissue on preoperative imaging reveals microvascular invasion in hepatocellular carcinoma: a systematic review and meta-analysis. *Abdom Radiol (NY)*. 2018;43(12):3324-3330. [CrossRef]
12. Huang J, Tian W, Zhang L, et al. Preoperative prediction power of imaging methods for microvascular invasion in hepatocellular carcinoma: a systemic review and meta-analysis. *Front Oncol*. 2020;10:887. [CrossRef]
13. Zhu F, Yang F, Li J, Chen WX, Yang WL. Incomplete tumor capsule on preoperative imaging reveals microvascular invasion in hepatocellular carcinoma: a systematic review and meta-analysis. *Abdom Radiol (NY)*. 2019;44(9):3049-3057. [CrossRef]
14. McInnes MDF, Moher D, Thombs BD, et al. Preferred reporting items for a systematic review and meta-analysis of diagnostic test accuracy studies: the PRISMA-DTA statement. *JAMA*. 2018;319(4):388-396. [CrossRef]
15. Moses LE, Shapiro D, Littenberg B. Combining independent studies of a diagnostic test into a summary ROC curve: data-analytic approaches and some additional considerations. *Stat Med*. 1993;12(14):1293-1316. [CrossRef]
16. Wang X, Zhang Z, Zhou X, et al. Computational quantitative measures of Gd-EOB-DTPA enhanced MRI hepatobiliary phase images can predict microvascular invasion of small HCC. *Eur J Radiol*. 2020;133:109361. [CrossRef]
17. Zhang L, Yu X, Wei W, et al. Prediction of HCC microvascular invasion with gadobenate-enhanced MRI: correlation with pathology. *Eur Radiol*. 2020;30(10):5327-5336. [CrossRef]
18. Zhang T, Pandey G, Xu L, et al. The value of TTPVI in prediction of microvascular invasion in hepatocellular carcinoma. *Cancer Manag Res*. 2020;12:4097-4105. [CrossRef]
19. Lee S, Kim KW, Jeong WK, et al. Gadoxetic acid-enhanced MRI as a predictor of recurrence of HCC after liver transplantation. *Eur Radiol*. 2020;30(2):987-995. [CrossRef]
20. Lu XY, Lu J, Zhang T, et al. Predicting microvascular invasion of hepatocellular carcinoma according to hepatobiliary stage peritumoral hypointensity during gadolinium-ethoxybenzyl-diethylenetriamine pentaacetic acid enhanced MRI. *Chin J Med Imaging Technol*. 2020;36:1350-1354
21. Chou YC, Lao IH, Hsieh PL, et al. Gadoxetic acid-enhanced magnetic resonance imaging can predict the pathologic stage of solitary hepatocellular carcinoma. *World J Gastroenterol*. 2019;25(21):2636-2649. [CrossRef]
22. Rhee H, An C, Kim HY, Yoo JE, Park YN, Kim MJ. Hepatocellular carcinoma with irregular rim-like arterial phase hyperenhancement: more aggressive pathologic features. *Liver Cancer*. 2019;8(1):24-40. [CrossRef]
23. Ahn SJ, Kim JH, Park SJ, Kim ST, Han JK. Hepatocellular carcinoma: preoperative gadoxetic acid-enhanced MR imaging can predict early recurrence after curative resection using image features and texture analysis. *Abdom Radiol (NY)*. 2019;44(2):539-548. [CrossRef]
24. Huang M, Liao B, Xu P, et al. Prediction of microvascular invasion in hepatocellular carcinoma: preoperative Gd-EOB-DTPA-dynamic enhanced MRI and histopathological correlation. *Contrast Media Mol Imaging*. 2018;2018:9674565. [CrossRef]
25. Kim AY, Sinn DH, Jeong WK, et al. Hepatobiliary MRI as novel selection criteria in liver transplantation for hepatocellular carcinoma. *J Hepatol*. 2018;68(6):1144-1152. [CrossRef]
26. Lee S, Kim SH, Lee JE, Sinn DH, Park CK. Preoperative gadoxetic acid-enhanced MRI for predicting microvascular invasion in patients with single hepatocellular carcinoma. *J Hepatol*. 2017;67(3):526-534. [CrossRef]
27. Zhou XM, Wang G, Gao YX, et al. Predict microvascular invasion in hepatocellular carcinoma by dynamic contrast-enhanced magnetic resonance imaging in patients with hepatitis B virus. *Int J Clin Exp Med*. 2017;10:11728-11738.
28. Yoneda N, Matsui O, Kitao A, et al. Peri-tumoral hyperintensity on hepatobiliary phase of gadoxetic acid-enhanced MRI in hepatocellular carcinomas: correlation with peri-tumoral hyperplasia and its pathological features. *Abdom Radiol (NY)*. 2018;43(8):2103-2112. [CrossRef]
29. Xu P, Zeng M, Liu K, Shan Y, Xu C, Lin J. Microvascular invasion in small hepatocellular carcinoma: is it predictable with preoperative diffusion-weighted imaging? *J Gastroenterol Hepatol*. 2014;29(2):330-336. [CrossRef]
30. Ahn SY, Lee JM, Joo I, et al. Prediction of microvascular invasion of hepatocellular carcinoma using gadoxetic acid-enhanced MR and (18) F-FDG PET/CT. *Abdom Imaging*. 2015;40(4):843-851. [CrossRef]
31. Kim KA, Kim MJ, Jeon HM, et al. Prediction of microvascular invasion of hepatocellular carcinoma: usefulness of peritumoral hypointensity seen on gadoxetate disodium-enhanced hepatobiliary phase images. *J Magn Reson Imaging*. 2012;35(3):629-634. [CrossRef]
32. Chandarana H, Robinson E, Hajdu CH, Drozhinin L, Babb JS, Taouli B. Microvascular invasion in hepatocellular carcinoma: is it predictable with pretransplant MRI? *AJR Am J Roentgenol*. 2011;196(5):1083-1089. [CrossRef]
33. Ariizumi S, Kitagawa K, Kotera Y, et al. A non-smooth tumor margin in the hepatobiliary phase of gadoxetic acid disodium (Gd-EOB-DTPA)-enhanced magnetic resonance imaging predicts microscopic portal vein invasion, intrahepatic metastasis, and early recurrence after hepatectomy in patients with hepatocellular carcinoma. *J Hepatobil Pancreat Sci*. 2011;18(4):575-585. [CrossRef]
34. Kim H, Park MS, Choi JY, et al. Can microvessel invasion of hepatocellular carcinoma be predicted by pre-operative MRI? *Eur Radiol*. 2009;19(7):1744-1751. [CrossRef]
35. Wang X, Wang W, Ma X, et al. Combined hepatocellular-cholangiocarcinoma: which preoperative clinical data and conventional MRI characteristics have value for the prediction of microvascular invasion and clinical significance? *Eur Radiol*. 2020;30(10):5337-5347. [CrossRef]
36. Matsui O, Kobayashi S, Sanada J, et al. Hepatocellular nodules in liver cirrhosis: hemodynamic evaluation (angiography-assisted CT) with special reference to multi-step hepatocarcinogenesis. *Abdom Imaging*. 2011;36(3):264-272. [CrossRef]
37. Zech CJ, Ba-Ssalamah A, Berg T, et al. Consensus report from the 8th International Forum for Liver Magnetic Resonance Imaging. *Eur Radiol*. 2020;30(1):370-382. [CrossRef]
38. Nishie A, Asayama Y, Ishigami K, et al. Clinicopathological significance of the peritumoral decreased uptake area of gadolinium ethoxybenzyl diethylenetriamine pentaacetic acid in hepatocellular carcinoma. *J Gastroenterol Hepatol*. 2014;29(3):561-567. [CrossRef]
39. Wu TH, Hatano E, Yamanaka K, et al. A non-smooth tumor margin on preoperative imaging predicts microvascular invasion of hepatocellular carcinoma. *Surg Today*. 2016;46(11):1275-1281. [CrossRef]
40. Chen J, Zhou J, Kuang S, et al. Liver imaging reporting and data system Category 5: MRI predictors of microvascular invasion and recurrence after hepatectomy for hepatocellular carcinoma. *AJR Am J Roentgenol*. 2019;213(4):821-830. [CrossRef]
41. Zhao W, Liu W, Liu H, et al. Preoperative prediction of microvascular invasion of hepatocellular carcinoma with IVIM diffusion-weighted MR imaging and Gd-EOB-DTPA-enhanced MR imaging. *PLoS One*. 2018;13(5):e0197488. [CrossRef]
42. Reginelli A, Vacca G, Segreto T, et al. Can microvascular invasion in hepatocellular carcinoma be predicted by diagnostic imaging? A critical review. *Future Oncol*. 2018;14(28):2985-2994. [CrossRef]
43. Sun SW, Liu QP, Xu X, Zhu FP, Zhang YD, Liu XS. Direct comparison of four presurgical stratifying schemes for prediction of microvascular invasion in hepatocellular carcinoma by gadoxetic acid-enhanced MRI. *J Magn Reson Imaging*. 2020;52(2):433-447. [CrossRef]
44. Zhu YJ, Feng B, Wang S, et al. Model-based three-dimensional texture analysis of contrast-enhanced magnetic resonance imaging as a potential tool for preoperative prediction of microvascular invasion in hepatocellular carcinoma. *Oncol Lett*. 2019;18(1):720-732. [CrossRef]
45. Feng ST, Jia Y, Liao B, et al. Preoperative prediction of microvascular invasion in hepatocellular cancer: a radiomics model using Gd-EOB-DTPA-enhanced MRI. *Eur Radiol*. 2019;29(9):4648-4659. [CrossRef]
46. Zhao J, Li X, Zhang K, et al. Prediction of microvascular invasion of hepatocellular carcinoma with preoperative diffusion-weighted imaging: A comparison of mean and minimum apparent diffusion coefficient values. *Med (Baltim)*. 2017;96(33):e7754. [CrossRef]

47. Li HX, Zhang J, Zheng ZY, et al. Preoperative histogram analysis of intravoxel incoherent motion (IVIM) for predicting microvascular invasion in patients with single hepatocellular carcinoma. *Eur J Radiol*. 2018;105:65-71. [CrossRef]

48. Rao C, Wang X, Li M, Zhou G, Gu H. Value of T1 mapping on gadoxetic acid-enhanced MRI for microvascular invasion of hepatocellular carcinoma: a retrospective study. *BMC Med Imaging*. 2020;20(1):43. [CrossRef]

49. Fan PL, Ding H, Mao F, Chen LL, Dong Y, Wang WP. Enhancement patterns of small hepatocellular carcinoma (≤30 mm) on contrast-enhanced ultrasound: correlation with clinicopathologic characteristics. *Eur J Radiol*. 2020;132:109341. [CrossRef]